**Figure 2.** Log–log representation of dependence of (a) EFA and (b) EFK upon the number of degrees of freedom $n - 2$ for $n$ data spanning 1.76 decades and taken at uniform time intervals. For large $n$, the limiting slope is −0.5. The details of the departure from this slope depend[9] upon the kind of noise and the decade range used. The corresponding results for EFA (a) for E noise and 0.88 decade coincide with the P curve. The corresponding results for EFK (b) for E noise and 0.88 decade are obtained by moving the curve for the P results up by log 2.

optimal decade range beyond which the added cost in time is not worth the resulting marginal reduction in the standard deviation.

Still other conditions are possible. For example, if the total number of counts is fixed, then, depending upon the number of time intervals, different optimal ranges are possible. This has been done for P noise with single photon counting in mind.[8]

**Effect of Number of Data on EFA and EFK**

The shapes of the curves in Figure 1 are relatively insensitive to the number of data used, but of course the values of $\sigma$ are affected thereby. The interpretation of the efficiency in terms of the fraction of wasted data has presumed that the product of the number of degrees of freedom $(n - 2)$ and the variance is a constant or $\sigma \sim 1/(n - 2)^{1/2}$ here. However, this dependence is only for very many data. For very large numbers of degrees of freedom the slope of the log $\sigma$ vs. log $(n - 2)$ would approach −0.5. For smaller $n$, the slope is less; this is shown in Figure 2a,b for 3–2100 data spanning 1.76 decades.[9] The results for E noise are not needed because they are related, for half the decade range, to the results for P noise, as noted above and in the captions, and

so are of identical slope. These results mean that doubling the number of degrees of freedom improves $\sigma$ by *less* than $2^{1/2}$ when $n - 2$ is not large. Similarly, having fewer data does not inflate $\sigma$ as much as it would if $n$ were large. In any case, one cannot vary $n$ at will. One important consideration involves the RC time constant of the measuring circuit. When this is an appreciable fraction of the time interval between successive data, the data become correlated and are no longer independent, as assumed when using NLLS: $n$ is effectively smaller.

This bears on the interpretation of efficiency given at the outset. Efficiency is defined in terms of the variances $(\sigma^2)$ and so to say that "an efficiency of 25% is equivalent to throwing out 75% of the data" is proper for large $n$ only. For smaller $n$, however, the equivalent waste of recorded data would be <75%.

**Conclusions**

The same computing power that facilitates nonlinear least-squares analyses also simplifies calculations with relative weights. We have found very large effects arising from the omission of relative weights on the precision of $A$ and $k$, for several common cases associated with the very widely followed exponential function. These quantiative results, for weighting and for the optimal decade range for the conditions noted, point to the profitability of experimenters devoting some time to establishing the kind of noise in their data and/or to considering just what decay range the data should span to better estimate parameters. Other reasons exist for extending the decay range, such as establishing a background reading or testing for a second exponential, but improving the precision of the extracted $k$ or $A$ is not generally one of them. The understanding of the relationship between efficiency and the use (or waste) of data we expend so much to collect should spur such investments and considerations. Table I and Figure 1 allow these considerations to be as quantitative as those made regarding the relative worth of introducing computer control of an experiment, insulating a home, etc. Finally, it should be noted that these results tell us nothing quantitative about the efficiencies of corresponding cases for other functions. Therefore, it would be prudent to investigate them in case such low efficiencies also occur for such apparently routine practices as ignoring the weights or being relatively arbitrary about the range spanned by data.

(8) Hall, P.; Selinger, B. K. *J. Phys. Chem.* **1981,** *85,* 2941.
(9) Guest, P. G. *Numerical Methods of Curve Fitting*; Cambridge University: Cambridge, England, 1961; Section 6.3.

# Depressing the Bistable Behavior of the Iodate–Arsenous Acid Reaction in a Continuous Flow Stirred Tank Reactor by the Effect of Chloride or Bromide Ions. A Method for Determination of Rate Constants

**V. Gáspár and M. T. Beck***

*Department of Physical Chemistry, Institute of Chemistry, Kossuth Lajos University,*
*Debrecen, Pf.7. 4010-Debrecen, Hungary (Received: May 27, 1986; In Final Form: July 15, 1986)*

Chloride or bromide ion catalysis of the iodate–iodide reaction causes changes in the location of the bifurcation point of the iodate–arsenous acid bistable system under continuous flow stirred tank reactor conditions. By the critical values of the halide ion concentrations, the rate constants of the catalyzed steps were determined: $3.2 \times 10^8$ and $3 \times 10^{10}$ M$^{-5}$ s$^{-1}$ in the case of chloride and bromide ions, respectively.

**Introduction**

Gray and Scott[1] showed in a series of publications that amplifying a bistable system based on a cubic autocatalysis (A +

(1) Gray, P.; Scott, S. K. *J. Phys. Chem.* **1985,** *89,* 22 and references cited therein.

2B → 3B) with a *decay* in the autocatalyst (B → C) may result in special patterns for dependence of the stationary state extent of conversion on residence time in a continuous flow stirred tank reactor (CSTR). In addition to the simple bistability, mushrooms, isolas, or even limit cycle oscillations might appear.

The first experimental demonstration of such patterns was given

by Ganapathisubramanian and Showalter.[2] They showed theoretically and experimentally the appearance of a mushroom and an isola in the iodate–arsenous acid bistable system[3,4] containing excess arsenous acid, when washing out was applied as a decay in the autocatalyst, iodide ion. In an earlier paper[5] they also demonstrated that under these experimental conditions there is a kind of a cubic autocatalysis, since the rate of the iodide autocatalysis is governed by the empirical rate law A[6] of the io-

$$R_A = \frac{d[I^-]}{dt} = \frac{-d[IO_3^-]}{dt} = (k_1 + k_2[I^-])[I^-][IO_3^-][H^+]^2 \quad (A)$$

date–iodide (Dushman[7]) reaction, where $k_1 = 4.5 \times 10^3$ M$^{-3}$ s$^{-1}$ and $k_2 = 4.5 \times 10^8$ M$^{-4}$ s$^{-1}$.[5] Furthermore, a simple third-order equation was derived to calculate the steady-state concentration of the iodide ion as a function of the residence time in the CSTR.

This simple treatment gave us the possibility to investigate the following problem. It is well-known that chloride[8–12] and bromide[12] ions increase the rate of the iodate–iodide reaction. Obviously, the promotion effect of a catalytic side reaction of the type

$$A + 2B \xrightarrow{\text{catalyst}} 3B \quad (R1)$$

(opposite of a decay) would not lead to new patterns in the iodate–arsenous acid system; however, it changes the location of the bifurcation point at which the bistable behavior of the system disappears.

The main goal of this paper is to point out how CSTR studies of such complicated systems might help to determine the rate constant of a catalytic side reaction and how these investigations support the effort to elucidate a mechanism for this reaction pathway.

According to the earlier investigations,[8–12] an overall rate law (B) for the iodate–iodide reaction in the presence of chloride or bromide ions in *batch* can be given as follows:

$$R_B = (k_1 + k_2[I^-] + k_3[H^+][X^-])[I^-][IO_3^-][H^+]^2 \quad (B)$$

where X = Cl$^-$ or Br$^-$ and $k_3 = 5.7 \times 10^8$ M$^{-5}$ s$^{-1}$ [9] for chloride ion. The value of $k_3$ for bromide ion is unknown, the steady-state concentration of iodide ion $[I^-]_s$ can be calculated in a buffered iodate–arsenous acid system, under CSTR conditions and at a constant inflow concentration of catalyst $[X^-]_0$ by the following algebraic equation:

$$k_2'[I^-]_s^3 - (k_2'S_0 - k_1' - k_3'[X^-]_0)[I^-]_s^2 -$$
$$(k_1'S_0 + k_3'S_0[X^-]_0 - k_0)[I^-]_s - k_0[I^-]_0 = 0 \quad (1)$$

where $k_1' = k_1[H^+]_0^2$, $k_2' = k_2[H^+]_0^2$, and $k_3' = k_3[H^+]_0^3$ and introducing $S_0 = [IO_3^-]_0 + [I^-]_0 = [I^-]_s + [IO_3^-]_s$. This equality follows from the fact that no other iodine-containing species is present in stoichiometrically significant concentrations when arsenite ion is in excess.

The well-known Descartes rule of signs gives a *necessary* requirement

$$K_2'S_0 > k_1' + k_3'[X^-]_0 \quad (2)$$

for having three positive real solutions of eq 1. Existence of a hysteresis loop is a consequence of the multistable behavior of the system. According to inequality 2, at the critical value of $[X^-]_0$
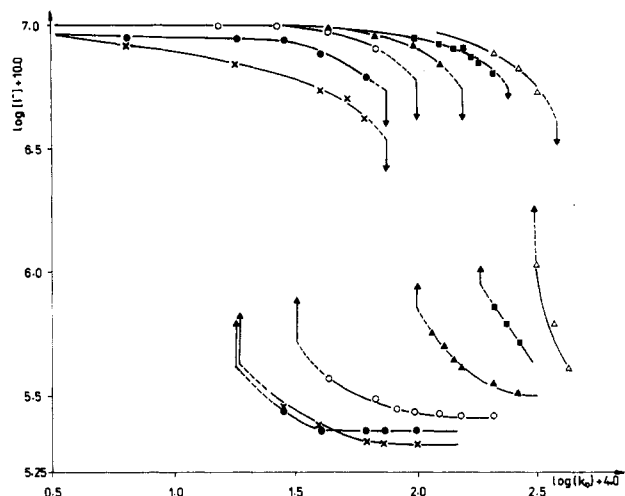
(2) Ganapathisubramanian, N.; Showalter, K. *J. Chem. Phys.* **1984**, *80*, 4177.

(3) Papsin, G. A.; Hanna, A.; Showalter, K. *J. Phys. Chem.* **1981**, *85*, 2575.

(4) DeKepper, P.; Epstein, I. R.; Kustin, K. *J. Am. Chem. Soc.* **1981**, *103*, 6121.

(5) Ganapathisubramanian, N.; Showalter, K. *J. Phys. Chem.* **1983**, *87*, 1098.

(6) Liebhafsky, H. A.; Roe, G. M. *Int. J. Chem. Kinet.* **1979**, *11*, 693.

(7) Dushman, S. *J. Phys. Chem.* **1904**, *8*, 453.

(8) Wronska, M.; Banas, B. *Rocz. Chem.* **1965**, *39*, 1745.

(9) Beran, P.; Bruckenstein, S. *J. Phys. Chem.* **1968**, *72*, 3630.

(10) Wilson, I. R. In *Comprehensive Chemical Kinetics*; Bamford, C. H., Tripper, C. F. H., Eds.; Elsevier: Amsterdam, London, New York, 1972; Vol. 6, p 383.

(11) Hirade, J. *Bull. Chem. Soc. Jpn.* **1935**, *10*, 97.

(12) Edwards, J. O. *Chem. Rev.* **1952**, *50*, 462.

**Figure 1.** Steady-state iodide concentration as a function of $k_0$ (reciprocal residence time) at different chloride ion concentrations: temperature 25 ± 0.1 °C; reactant stream concentrations, [As(III)]$_0$ 5.0 × 10$^{-3}$ M; [IO$_3^-$]$_0$ 1.0 × 10$^{-3}$ M; [I$^-$]$_0$ 2.0 × 10$^{-5}$ M; [H$^+$]$_0$ 6.9 × 10$^{-3}$ M (buffered with 0.02 M HSO$_4^-$/0.04 M SO$_4^{2-}$ buffer); [Cl$^-$]$_0$ (●) 0.00 M, (×) 10$^{-3}$ M, (○) 10$^{-2}$ M, (▲) 5 × 10$^{-2}$ M, (■) 10$^{-1}$ M, (△) 0.15 M; CSTR volume, 60.0 mL in the case [Cl$^-$] = 0 and 10$^{-3}$ M, while 25.0 mL in other cases.
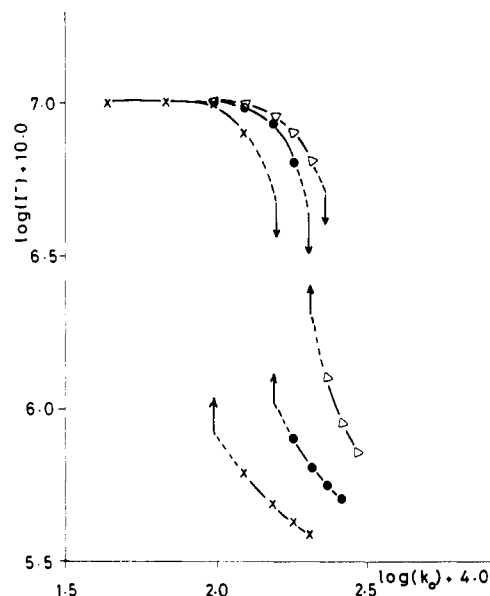


**Figure 2.** Steady-state iodide concentration as a function of $k_0$ at different bromide ion concentrations. Reactant stream concentrations are the same as in Figure 1. CSTR volume, 25 mL. [Br$^-$]$_0$ (×) 10$^{-3}$ M, (●) 1.5 × 10$^{-3}$ M, (▽) 2 × 10$^{-3}$ M; temperature, 25 ± 0.1 °C.

the hysteresis loop disappears. Measuring this value experimentally can determine the rate constant $k_3$.

## Materials and Equipment

All chemicals were reagent grade (Reanal products). Iodate solutions were prepared by dissolving KIO$_3$ in doubly distilled water buffer containing 0.2 M NaHSO$_4$ and 0.04 M Na$_2$SO$_4$ (pH 2.16). The procedure for preparing the second feed solution was the following: As$_2$O$_3$ was dissolved in water containing a stoichiometrically equivalent amount of NaOH. The final concentration of Na$_2$SO$_4$ was adjusted by adding the required amount of H$_2$SO$_4$ for neutralization and then by dissolving a further amount of Na$_2$SO$_4$. Finally, the calculated amounts of NaHSO$_4$·H$_2$O, KI, and KCl (or KBr) were dissolved in this solution. The actual reactant stream concentrations are given in Figures 1 and 2.

The tank reactor was constructed of two pieces machined from a thermostated glass vessel and a Vinidur (PVC-based) top. Reactant solutions were pumped through two capillary tubings (Cole-Palmer 6408-41, Tygon) to the CSTR with a Cole-Palmer

peristaltic pump at the top section. The solution was stirred with a magnetic stirrer. A number of different-sized Vinidur O-rings allowed the variation of tank volume. The solution was continuously drained by a water pump. The top section was designed to accommodate an iodide-selective electrode (Radelkis OP-I-O711P) and a salt bridge. The reference was a saturated calomel electrode (Radiometer K401) connected to the system by a double junction salt bridge (saturated KNO$_3$–saturated KCl). The electrodes were connected to a Radiometer PHM 51 millivolt-meter. The iodide concentration as a function of time was recorded with a Radelkis OH-814/1 recorder.
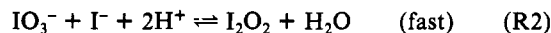
**Results**

Steady-state iodide concentration as a function of $k_0$ (reciprocal residence time) at different chloride concentrations is shown in Figure 1. The results demonstrate that on increasing chloride concentration the region of hysteresis becomes more and more narrow. This is in good agreement with the predictions, qualitatively. Drawing the experimentally found region of hysteresis ($\Delta \log k_0$) as a function of chloride concentration gives by extrapolation the upper limit of [Cl$^-$] for bistability. ([Cl$^-$] limit equals 0.2 M.) Although this extrapolation shows high uncertainty, it follows from inequality 2 that the value of $k_3'$ has to be less than $3.2 \times 10^8 [\mathrm{H^+}]_0^3$ s$^{-1}$. This value differs only by less than a factor of 2 from the value determined by Beran and Bruckenstein.[9] The reason can be the different ionic strengths applied.

Figure 2 shows that the effect of bromide is more remarkable than that of chloride ion. The critical concentration of bromide ion is much lower ($2 \times 10^{-3}$ M). As a consequence, the $k_3'$ value
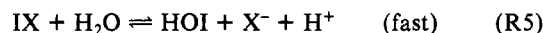
for bromide ion is higher by at least 2 orders of magnitude ($3 \times 10^{10}[\mathrm{H^+}]_0^3$ s$^{-1}$) than the analogous value for chloride ion.

The agreement between the $k_3'$ values for chloride ion catalysis under batch and CSTR conditions justifies also the rate equation B. The halide ion catalysis term in the rate equation is consistent with the mechanism given by Edwards[12] earlier

$$\mathrm{IO_3^- + I^- + 2H^+ \rightleftharpoons I_2O_2 + H_2O} \qquad \text{(fast)} \qquad \text{(R2)}$$

$$\mathrm{I_2O_2 + X^- + H^+ \xrightarrow{k_3} IX + HIO_2} \quad \text{(rate determining)} \qquad \text{(R3)}$$

although other alternatives might also be possible. This explanation is in good agreement with the detailed mechanism of the iodate–iodide reaction given by Bray,[13] confirmed by Liebhafsky and Roe,[6] and applied by Papsin et al.[3] as a part of the detailed mechanistic description of the iodate–arsenous acid reaction in CSTR.

The regeneration of the halide ion might occur by either of the following processes:

$$\mathrm{IX + I^- \rightleftharpoons I_2 + X^-} \qquad \text{(fast)} \qquad \text{(R4)}$$

$$\mathrm{IX + H_2O \rightleftharpoons HOI + X^- + H^+} \qquad \text{(fast)} \qquad \text{(R5)}$$

(13) Bray, W. C. *J. Am. Chem. Soc.* **1930**, *52*, 3580.

# Secondary Reactions following Flash Photodissociation of Iodoethane and 1-Iodopropane

**David M. Hayes**

*Department of Chemistry, Union College, Schenectady, New York 12308*

**and Robert L. Strong\***

*Department of Chemistry, Rensselaer Polytechnic Institute, Troy, New York 12180-3590*
*(Received: April 28, 1986)*

The room-temperature rate constant for the reaction R + I$_2$ → RI + I has been determined from a series of consecutive flash photodissociations of the appropriate iodoalkane in 200 Torr SF$_6$ and the accumulated I$_2$. For both C$_2$H$_5$ and *n*-C$_3$H$_7$ radicals, $k = (5 \pm 1) \times 10^{-11}$ cm$^3$ molecule$^{-1}$ s$^{-1}$, an order of magnitude greater than previously reported. When included with other kinetic parameters from thermal iodination studies, this larger rate constant leads to a heat of formation for the ethyl radical of $\Delta H_f^{\ominus}{}_{298}(\mathrm{C_2H_5}) = 27.8 \pm 0.8$ kcal mol$^{-1}$.

**Introduction**

The photochemistry of the alkyl iodides has been extensively studied over the course of several decades. The maximum of the broad UV absorption band in the simple alkyl iodides, corresponding to an n → $\sigma^*$ transition localized on the carbon–iodine bond, lies near 257 nm. Absorption here leads to prompt dissociation of the alkyl iodide (in at least 0.065 ps for iodomethane[1])

$$\mathrm{RI} + h\nu \rightarrow \mathrm{R} + x\mathrm{I^*} + (1-x)\mathrm{I} \qquad (1)$$
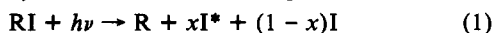
where I represents atomic iodine in its ground ($^2\mathrm{P}_{3/2}$) electronic state and I\* represents the iodine atom in its first excited, spin–orbit ($^2\mathrm{P}_{1/2}$) state. The branching ratio I\*/(I\* + I) varies with the alkyl iodide, from <0.1 for 2-iodopropane to a high of >0.99

for 1-iodoheptafluoropropane. For iodoethane and 1-iodopropane the branching ratios are 0.69 ± 0.05 and 0.67 ± 0.04, respectively.[2]

In 1964 Kasper and Pimentel[3] reported that the population inversion involving ground and excited iodine atoms created by reactions of the above type had been observed to give laser emission. This was the first laser in which inversion is achieved by photodissociation. The energy difference between the ground and first excited electronic states of the iodine atom is 91 kJ/mol, which corresponds to a transition wavelength of 1315 nm. The development of the iodine atom laser has proceeded rapidly, in large part because of its potential applicability in high-gain inertial confinement fusion reactors.[4]

(1) Dzvonik, M.; Yang, S.; Bersohn, R. *J. Chem. Phys.* **1974**, *61*, 4408.

(2) Donohue, T.; Wiesenfeld, J. R. *J. Chem. Phys.* **1975**, *63*, 3130.
(3) Kasper, J. V. V.; Pimentel, G. C. *Appl. Phys. Lett.* **1964**, *5*, 231.